Molecular Cell

Volume 2 Number 1 July 1998

Hexameric RNA in Phage Packaging

Molecular Cell, Vol. 2, 149–155, July, 1998, Copyright ©1998 by Cell Press

Inter-RNA Interaction of Phage ϕ29 pRNA to Form a Hexameric Complex for Viral DNA Transportation

Peixuan Guo,* Chunlin Zhang, Chaoping Chen, Kyle Garver, and Mark Trottier
Department of Pathobiology
Purdue Biochemistry and Molecular Biology Program
Purdue University
West Lafayette, Indiana 47907

Summary

Ds-DNA viruses package their DNA into a preformed protein shell (procapsid) during maturation. Bacteriophage ϕ29 requires an RNA (pRNA) to package its genomic DNA into the procapsid. We report here that the pRNA upper and lower loops are involved in RNA/RNA interactions. Mutation in only one loop results in inactive pRNAs. However, mixing of two, three and six inactive mutant pRNAs restores DNA packaging activity as long as an interlocking hexameric ring can be predicted to form by base pairing of the mutated loops in separate RNA molecules. The stoichiometry of pRNA for the packaging of one viral DNA genome is six. Homogeneous pRNA purified from a single band in denaturing gels showed six bands when rerun in native gels. These results suggest that six pRNAs form a hexameric ring by the intermolecular interaction of two RNA loops to serve as part of the DNA transportation machinery.

Introduction

Migration or translocation of macromolecules through barriers is a common process in biological systems. After transcription, mRNA and tRNA must pass the nuclear membrane to reach the translation machinery in the cytoplasm. Similarly, nuclear proteins must pass from the cytoplasm, where they are synthesized, to the nucleus, where they function. After infection or transfection, most viral or plasmid DNA must pass the nuclear membrane to serve as template for gene expression (reviewed in Davis, 1995). The Rev protein of HIV helps in the translocation of viral mRNA from the nucleus to the cytoplasm through a nuclear pore (Pfeifer et al., 1991; Krug, 1993). Varieties of proteins and other elements migrate into and out of the cell and nucleus to perform their respective functions. Molecular migration or translocation also is manifest in the tracking and rail riding of enhancers or transcriptional factors along DNA (Herendeen et al., 1992), the translocation of the transcription termination protein Rho along RNA (Geiselmann et al., 1993), and the migration of helicases along single-stranded DNA during DNA replication (Egelman, 1996; West, 1996; San Martin et al., 1997).

One of the most complex and intricate translocation processes is viral DNA encapsidation. All linear ds-DNA viruses, including hepesviruses, poxviruses, adenoviruses, and the ds-DNA bacteriophages, package their genomic DNA into a procapsid. ATP provides energy to condense the lengthy genomic DNA into the limited space inside procapsids with remarkable velocity. Phage ϕ29 requires a viral-encoded RNA (pRNA) to package its genomic DNA (Guo et al., 1987a, 1987b). This pRNA binds to the connector of procapsids (the unique site on procapsids where DNA enters and exits) (Guo et al., 1986, 1987b; Chen and Guo, 1997b) as the first step in DNA packaging. Procapsids with pRNA attached are competent to be converted into DNA-filled heads with the aid of the DNA packaging protein gp16 and ATP. The pRNA secondary structure (Figure 1A) has been proposed by phylogenetic analysis (Bailey et al., 1990) and partially confirmed (Bailey et al., 1990; Reid et al., 1994b; Zhang et al., 1994, 1995b, 1997). Two domains within the pRNA have also been identified, one in the middle of the sequence for connector binding, and the other at the 5′/3′ paired ends that has an unknown yet essential role in DNA packaging, so called the "DNA translocation" domain (Figure 1A) (Reid et al., 1994a, 1994b; Zhang et al., 1994, 1995a; Trottier et al., 1996; Garver and Guo, 1997). A Mg^{++}-induced conformational change in the pRNA leads to its binding to the connector (Chen and Guo, 1997b). A pseudoknot within the pRNA was predicted to form by the pairing of bases 45–48 with bases 85–82, respectively (Reid et al., 1994b).

Previous work has indicated that approximately six pRNAs are attached to procapsids (Wichitwechkarn et al., 1989; Reid et al., 1994a). We have shown that several pRNAs with mutations in the 5′/3′-terminal helix were inactive in ϕ29 DNA packaging but were still able to bind procapsids with wild-type affinity (Zhang et al., 1994; Reid et al., 1994b; Trottier et al., 1996; Garver and Guo, 1997; Trottier and Guo, 1997). These mutant pRNAs were able to inhibit ϕ29 assembly efficiently in vitro and in vivo (Trottier et al., 1996). Competition inhibition assay with these mutants also indicated that 5–6 copies of pRNA are needed for DNA packaging (Trottier and Guo, 1997).

The pRNA is not part of the mature ϕ29 virion and leaves the procapsid after DNA packaging is completed (Chen and Guo, 1997a), implying participation of the pRNA in the DNA translocation process. The pRNA appears to contribute to the ATPase activity associated with DNA packaging (Grimes and Anderson, 1990) (M. T. and P. G., unpublished data). We reported that one ATP is needed for the packaging of two base pairs of ϕ29 DNA (Guo et al., 1987c), suggesting that DNA is driven into the capsid by some type of ATPase motor (reviewed by Guo and Trottier, 1994; Doering et al., 1995).

In this paper, we report an intermolecular interaction of pRNA through base pairing between the upper loop (bases 45–48) and the lower loop (bases 85–82). Evidence for the formation of a pRNA hexameric ring due to this intermolecular pairing is reported.

Results

Intermolecular Interaction between the Upper and Lower Loops of pRNAs

The secondary structure of the pRNA is shown in Figure 1A. We show in this report that the upper and the lower

*To whom correspondence should be addressed (e-mail: guo@vet.purdue.edu).

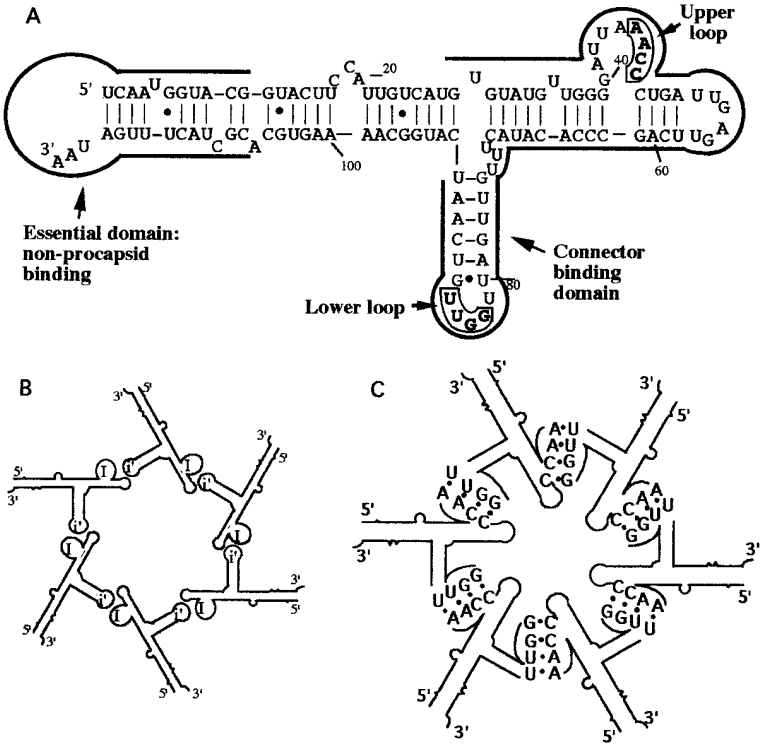

Figure 1. Structure of pRNA and Hexamer Formation

(A) Sequence and predicted secondary structure of wild-type pRNA. Two domains, the connector binding domain and the DNA translocation domain, are marked with bold lines, and the four bases in the upper and lower loops responsible for inter-RNA interactions are boxed and in bold type.

(B and C) Diagrams depicting the formation of a pRNA hexameric ring by upper loop sequence I, 5′-AACC, and lower loop sequence i′, 3′-UUGG, interaction.

loops paired intermolecularly instead of intramolecularly, implying that the two loops interact during DNA packaging (Figures 1B and 1C). We have constructed more than 200 mutant pRNAs with alterations in the upper and lower loops (our unpublished data). Here, the uppercase and lowercase letters are used to represent the upper and lower loop sequences, respectively (Table 1). The same letter in upper- and lowercase represents a pair of complementary sequences. For example, in pRNA J–j′, the upper loop sequence J (5′-CCGU-3′) and lower loop sequence j′ (3′-GGCA-5′) are complementary; while in pRNA J–i′, the upper loop sequence J is not complementary to the lower loop sequence i′ (3′-UUGG-5′). The sequences representing the four bases of each mutant loop are listed in Table 1. All pRNAs that had mutations resulting in unpaired upper and lower loops, such as pRNA J–i′, were inactive in in vitro ϕ29 assembly when used alone. However, when two inactive pRNAs that were transcomplementary in their upper and lower loops, for example pRNA I–j′ and J–i′, were mixed in a 1:1 molar ratio, full activity was restored (Table 2, VI). The presence of mutant pRNA without transcomplementary loop(s) did not interfere with assembly mediated by pRNAs with transcomplementary loops (data not shown). Since a closed ring composed of an even number of pRNAs can form from two mutant pRNAs with interlocking upper and lower loop sequences, it suggests that I–j′ and J–i′ interact or form a complex via intermolecular interaction of the upper and lower loops. The observed activity of a mixture of two inactive mutants (Table 2) suggests that the number of pRNAs in the DNA packaging complex was a multiple of two.

Table 1. Upper and Lower Loop Sequences of Mutant pRNAs

A 5'-GGAC-3' a' 3'-CCUG-5'	F 5'-AGAC-3' f' 3'-UCUG-5'
B 5'-ACGC-3' b' 3'-UGCG-5'	I 5'-AACC-3' i' 3'-UUGG-5'
C 5'-GACA-3' c' 3'-CUGU-5'	J 5'-CCGU-3' j' 3'-GGCA-5'
D 5'-AGGC-3' d' 3'-UCCG-5'	K 5'-UCCU-3' k' 3'-AGGA-5'
E 5'-GCCA-3' e' 3'-CGGU-5'	P 5'-CUAC-3' p' 3'-GAUG-5'

Another set of mutants composed of the three mutant pRNAs, J–p′, P–k′, and K–j′, was also constructed. This set contains interlocking sequences that are predicted to be able to form a 3-, 6-, 9-, or 12-mer ring that carries each of the three mutants. When pRNAs J–p′, P–k′, or K–j′ were tested alone, each individual pRNA showed little or no activity (Table 2, VII, VIII, and IX). When any two of the three mutant pRNAs were mixed together and tested by in vitro phage assembly assays, again little or no activity was detected (Table 2, X, XI, and XII). The fact that activity cannot be detected with the combination of two of the mutants can be interpreted by the inability to form a closed ring with any two of these three mutant pRNAs. However, when all three pRNAs were mixed in a 1:1:1 ratio, DNA packaging activity was restored (Table 2, XIV). The lack of activity of

Table 2. Inter-pRNA Interaction of Two Loops

pRNAs	Activity (pfu/ml)	Predicted Hexamer
I. I-i' (wild type pRNA alone)	8×10^7	Active (I)
II. J-j' (Compensatory modification)	7×10^7	Active (II)
III. J-i' (Mutation with unpaired loop)	0	Inactive (III)
IV. I-j' (Mutation with unpaired loop)	0	Inactive (IV)
V. (I-j')+(J-p') (miss one link)	0	Inactive (V)
VI. (I-j') + (J-i') (Compensatory pair)	4×10^7	Active (VI)
VII. J-p' (Mutation with unpaired loop)	0	Inactive (VII)
VIII. P-k' (Mutation with unpaired loop)	0	Inactive (VIII)
IX. K-j' (Mutation with unpaired loop)	0	Inactive (IX)
X. (J-p') + (P-k') (miss one link)	5×10^3	5×10^3 (X)
XI. (P-k') + (K-j') (miss one link)	0	Inactive (XI)
XII. (K-j') + (J-p') (miss one link)	0	Inactive (XII)
XIII. (J-p') + (P-k') + (K-a') (miss one link)	1×10^4	1×10^4 (XIII)
XIV. (J-p') + (P-k') + (K-j') (compensatory trimer)	1×10^7	Active (XIV)
XV. (A-b')+(B-c') + (C-d')+(D-e') + (E-f')+(F-a') (hexamer)	2×10^7	Active (XV)

Diagram showing interaction of the pRNA upper and lower loops serving as bridges for hexamer formation. The uppercase letter stands for the upper loop and lowercase for the lower loop. The same letter in upper- and lowercase represents two sequences that are complementary. The "||" at the vertices indicate that two loops are noncomplementary. See Table 1 for loop sequences.

mixtures of two and the restored activity of mixtures of three of the three mutant pRNAs was expected since the mutations in each RNA were engineered such that only the presence of all three RNAs would produce a closed ring (Table 2, XIV). The fact that three inactive pRNAs were fully active when mixed together suggests that the number of pRNAs in the DNA packaging complex was a multiple of 3, in addition to being a multiple of two. Thus, the number of pRNAs required for DNA packaging is a common multiple of 2 and 3, which is 6 (or 12, but this number was excluded by the experiment described below). DNA packaging activity was also achieved by mixing six mutant interlocking pRNAs, each being inactive when used alone but was predicted to form a hexameric ring when mixed (Table 2, XV). These results strongly suggest that pRNAs interact intermolecularly through base pairing of the upper and lower loops during DNA translocation.

Hexamer Formation Was Supported by Stoichiometry Determination Using Competition Inhibition Method

As reported above, the number of pRNAs needed for the packaging of one viral genome is a common multiple of 2 and 3, that is, either 6 or 12. Here we use a similar competition inhibition method (Trottier and Guo, 1997) and newly constructed mutant pRNAs to determine whether the pRNA stoichiometry is 6 or 12. Mutant pRNA B–a′CCA, in which the $C_{18}C_{19}A_{20}$ bulge has been eliminated by insertion of three bases 5′-UGG between A_{99} and A_{100} (Figure 1), has previously been shown to retain wild-type procapsid binding affinity while having no DNA packaging function (Zhang et al., 1997). When variable ratios of B–a′CCA and B–a′ were mixed with A–b′ (in which the total amount of B–a′ plus B–a′CCA equaled the total amount of A–b′) and used in in vitro ϕ29 assembly assays (i.e., 50% A–b′, 10% B–a′CCA, and 40% B–a′, with a constant total amount of pRNA in each assembly assay), the probability that a procapsid would possess a certain number of B–a′CCA and a certain number of B–a′ was predicted with a binomial (see Experimental Procedures and Trottier and Guo, 1997). The yield of virions from empirical data was plotted and compared to a series of predicted curves to find a best-fit (Figure 2). The rationale behind this experimental design is that, if our conclusion concerning the interaction of the upper and the lower loops to form a hexameric complex is valid, each procapsid should contain three copies of

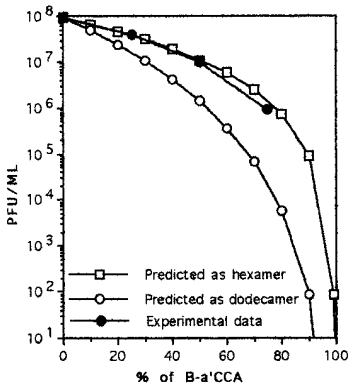

Figure 2. Distinguishing the Stoichiometry of the ϕ29 pRNA in DNA Packaging between 6 and 12 Copies

Predicted and empirical curves of the percentage of mutant pRNA B-a′CCA were plotted against the yield of infectious virions in in vitro phage assembly assays, expressed as pfu/ml. Virion assembly was performed in the presence of pRNA A-b′, B-a′, and B-a′CCA. Predictions were made with the binomial equation (see Experimental Procedures), assuming that the total pRNA number per procapsid, Z, is equal to 6 (open squares), or 12 (open circles). The experimental data (solid circles) fits to Z = 6.

A–b′ and three copies of B–a′ and/or B–a′CCA, where the copy number of B–a′CCA incorporated into each procapsid can be predicted based on the percentage of B–a′CCA present in the reaction mixture. Only those procapsids that have three A–b′ and three B–a′ could produce infectious particles, while those that have one or more B–a′CCA would not. Two theoretical curves were predicted with the assumption that the pRNA ring is composed of 6 or 12 pRNAs, respectively. The empirical curve most closely matched, in both slope and magnitude, the curve predicted for 6 copies of pRNA per procapsid, not 12 copies (Figure 2), supporting the formation of a hexameric ring. We used an even number of mutated interlocking pRNA in this experiment. The possibility of five or seven copies of the pRNA being required for DNA packaging can be excluded since the conclusion must be an even number.

Formation of a Single Band in Denaturing Gels and Multiple Bands in Native Gels

To attempt to visualize pRNA hexamers, pRNA 7/11 (Zhang et al., 1994) was purified from denaturing gels after in vitro transcription (Figure 3A). 7/11 retained the packaging activity of wild-type pRNA while containing two mutations at the 5′ and 3′ ends to facilitate transcription with T7 RNA polymerase and to maintain the secondary structure of wild-type pRNA. After reloading onto a 10% native gel containing Mg^{++} (Figure 3B), a ladder of six bands that may represent monomers, dimers, trimers, tetramers, pentamers, and hexamers of the pRNA, respectively, was observed. A plot of the log molecular weight versus migration distance of each band showed that the bands, from fastest to slowest migrating, were proportional to molecular weight multiples of 1:2:3:4:5:6, respectively (Figure 3III). Each of these bands was isolated from the gel and purified, and shown to be fully active in DNA packaging (data not shown). Bands representing pRNA oligomers (slower-migrating bands) ran as

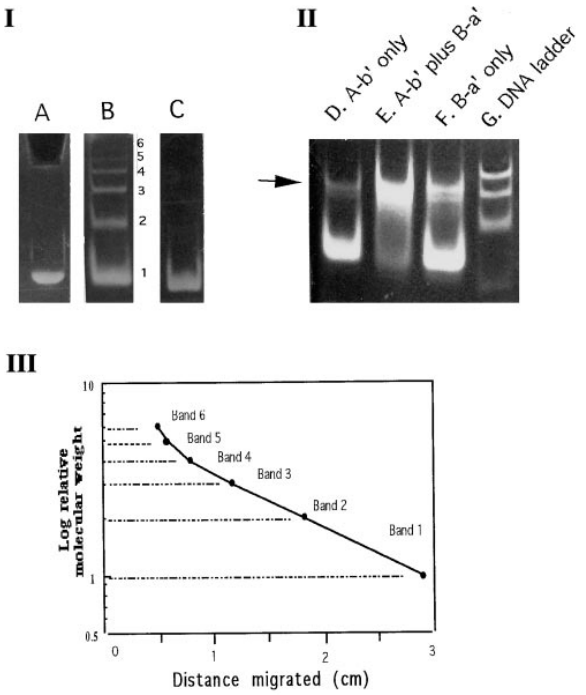

Figure 3. Formation of pRNA Oligomers Shown by Native Polyacrylamide Gel

pRNA 7/11 was purified to homogeneity shown as one band in the denaturing gel (A) and rerun under native conditions (B), which showed 6 bands that may represent monomer, dimer, trimer, tetramer, pentamer and hexamer, respectively. In native gel only one band was detected for pRNA A-b′ with unpaired upper and lower loops (C). pRNA complex formation was demonstrated in native gel by mixing pRNA A-b′ and B-a′ (E). When mixed, both A′-b′ and B-a′ were shifted to a band with migration rate slower that the band for pRNA A-b′ (D) or B-a′ (F) alone. (III) shows correlation between molecular weights of multimers and their migration distances, given that the multiple bands in (B) are monomer, dimer, trimer, tetramer, pentamer, and hexamer, respectively. A smooth line was observed that agreed with the typical distance versus log molecular weight plot.

monomers when rerun in Mg^{++}-free buffer. Additionally, nonspecific RNA showed no apparent oligomerization either in Mg^{++} or Mg^{++}-free gels (data not shown). Consequently, Mg^{++} may play a role in the formation of pRNA complexes, potentially by stimulating loop interactions or directing proper pRNA folding. When mutant pRNA A–b′, with the upper and lower loops predicted to be unpaired, was purified and reloaded onto a native Mg^{++} gel, only one band was detected (Figure 3C), again indicating that an interaction between the upper and lower loops plays a role in the formation of pRNA complexes.

The conclusion of an interaction between the upper and lower loops of different pRNA molecules was also strongly supported by the shift of pRNA migration rate in native gels when circularly permuted (Zhang et al., 1995c, 1997) pRNA A–b′ was mixed with B–a′ (Figure 3). A shift to a slower-migrating band was seen when both RNAs were run together, while very little shift was observed when each RNA was alone. Whether the band with the slower migration rate represented a hexamer or dimer remains to be investigated.

Discussion

In this paper the interaction of upper and lower loops is reported to involve only four bases. Our extensive investigation found that two GC pairs in the loops were sufficient to provide the pRNA with assembly activity (our unpublished data). However, we expect that the tertiary structure of the environment around the loops might contribute to inter-RNA interaction and the stability of the hexameric complex. This expectation is also supported by the evidence that some incorrect pairs were able to program up to four logs of phage assembly, albeit several logs less than the correct pair (Table 2, X and XIII). Though the residual activity might be interpreted by non–Watson-Crick base pairings or tolerated mismatches, the pairing of only four bases or mismatch pairing may not be strong enough to hold a stable RNA complex without the help of the three-dimensional neighboring environment. This system might provide a unique model for the study of RNA complex formation through a new mechanism of hand-in-hand interaction of two loops of each RNA molecule. These two loops could be called "left" and "right" "hand-in-hand loops" to distinguish them from psuedoknots and kissing loops.

The formation of a pRNA "ring" is not unfeasible as the pRNA is already known to bind to the connector of the phage procapsid. The connector is located at a unique vertex of the icosahedral head and is the site where DNA enters and exits the capsid and where the phage tail attaches. These connectors are ring-like, oligomeric structures containing an axial hole large enough to accommodate ds-DNA passage (Ibanez et al., 1984; 1984; Michaud et al., 1989; Rishovd et al., 1994). Recent electron microscopy studies have indicated that the connector is a ring that has either 12- (Jimenez et al., 1986) or 13-fold symmetry (Dubé et al., 1993; Tsuprun et al., 1994).

An immediate question is to inquire of the role of the connector, or procapsid, in the formation of a pRNA hexamer. Three possible pathways of RNA hexamer formation could exist. The first pathway is that a pRNA hexamer is preformed before attaching to the procapsid. The second one is that a dimeric pRNA is preformed and only the dimeric pRNA could bind to the procapsid. After the binding of one dimer to procapsids, two more dimers are recruited by sequential interaction of the interlocking loops. The third pathway is that a hexamer is formed by the sequential addition of monomeric pRNA to the connector of procapsids, and interlocking loops serve to recruit the neighboring pRNA. Though the third pathway can be ruled out by data in this report and our unpublished results, there is no sufficient data to confirm that a hexamer can form with complete independence from the procapsid. It is important to note that the pRNA does not perform its biological function alone. Rather, the pRNA acts in concert with the ϕ29 procapsid and gp16 to form an ATPase motor for DNA packaging. Indeed, the first step in ϕ29 DNA packaging is the binding of the pRNA to the connector of procapsids. Consequently, it is possible that the pRNA does form a hexamer, but requires procapsid binding to stabilize the hexamer structure. It is also possible that the equilibrium

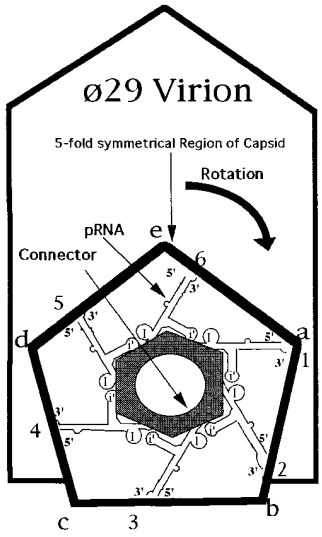

Figure 4. A Diagram Depicting the Location and a Possible Role of the Hexameric pRNA Complex in ϕ29 DNA Translocation

The shaded hexagon represents the connector and the surrounding pentagon represents the five-fold symmetrical capsid membrane, viewed as end-on with the virion as side-view. The six protrusions represent six pRNAs with the central region bound to the connector and the 5′/3′ paired region extending outward. It is proposed that a symmetry mismatch between five- and six-fold symmetry could reduce the energy barrier if rotation at this interface occurs, and provides an opportunity for each pRNA (1–6) to pass the vertex (a to e) of the pentagon alternately and sequentially. Similar to the motion of myosin in muscle, alternating contraction and relaxation of the pRNA, or other DNA packaging components bound to the connector, could provide a physical force to drive connector rotation. Sequential conformational changes of pRNAs driven by ATP hydrolysis, and/or induced by Mg^{++}, might provide a force to rotate the connector relative to the capsid shell. As a result of rotation, DNA-gp3 is screwed into the procapsid either through the central hole of the connector or wrapping around the outside of the connector (for more details of the model, please see Chen and Guo, 1997a).

constant for hexamer formation favors pRNA monomers and oligomers over hexamers. Thus, if the hexamer is the functional form of the pRNA that binds procapsids, hexamer binding to procapsids would drive the equilibrium toward hexamer formation in the presence of procapsids. The significant band shift in Figure 3E might argue for the existence of inter-pRNA interaction independent of procapsid; however, it cannot argue against pathway two since we still do not know whether slower-migrating bands in native gels represent dimer or hexamer. Nevertheless, pRNA was able to form a complex, at least a dimer, in solution without the involvement of any proteins.

The capsid of ϕ29, as well as other icosahedral phages, contain a 5-fold symmetrical region where the connector sits, thus a 5-fold/6-fold symmetry mismatch exists at the connector/capsid interface. A model was previously proposed speculating that a symmetry mismatch could reduce the energy barrier if rotation at this interface occurs (Hendrix, 1978; Chen and Guo, 1997a). To make the connector rotate in such a manner, at least one additional component is needed to provide a propelling force. Since the pRNA binds to the connector (Guo et al., 1987a; Chen and Guo, 1997b; Garver and Guo,

1997), it could be a candidate for this third component. With two functional domains, the pRNA is able to bind to the connector with its central domain, leaving a free 5′/3′ essential domain that may interact with an additional component. Interaction of the pRNA, which is tethered to the connector, with the capsid or genomic DNA could provide a propelling force for connector rotation (Figure 4). Similar to the motion of myosin in muscle, alternating contraction and relaxation of the pRNA, or other DNA packaging components bound to the connector, could provide a physical force to drive connector rotation. Indeed, we have reported that one ATP is needed for the packaging of two base pairs of ϕ29 DNA (Guo et al., 1987c). Direct evidence of contraction and relaxation could come from the observation of conformational changes. We also found that both ATP (our unpublished data) and Mg^{++} (Chen and Guo, 1997b) induce conformational changes in the pRNA. These conformational changes may have relevance to those predicted to be involved in connector rotation.

ATP hydrolysis is proposed to drive the sequential conformational changes that drive the putative connector rotation (Chen and Guo, 1997a). Analogous to the sequential action of six cylinders in a car engine, sequential action of six pRNAs is one way to achieve the turning of this DNA packaging motor. If the six cylinders fired synchronously, the engine would not run continuously. Our previous report that six pRNAs work sequentially (Chen and Guo, 1997a) supports the connector rotation hypothesis. The intermolecular interaction of ϕ29 pRNAs reported here strongly supports the mechanism of pRNA sequential action reported (Chen and Guo, 1997a). For six pRNAs to act sequentially, the pRNAs may need to communicate to ensure that the packaging process progresses in a consecutive manner. Inter-pRNA interactions, through the upper and lower loops, might serve as a link to pass a signal to adjacent pRNAs. Base pairing would allow such a signal to pass while unpaired bases would break the chain and result in aborted DNA packaging. A signal, possibly via subtle conformational shifts, would ensure that only one of the six pRNAs bound to the connector would be in the "active" conformation (Figure 4). Thus, base pairing between the upper and lower loops might be necessary to transfer the conformational change from one pRNA to an adjacent one.

The process of molecular motion has been the subject of intense scrutiny. Recent studies on DNA or RNA translocation enzymes have shed new light on the mechanism of migration involving nucleic acids. The gate for DNA entry into phage procapsids is the connector. It appears that several similarities exist between the DNA encapsidation process of ds-DNA viruses and other cellular translocation process. Translocating enzymes, such as DNA helicases (Egelman, 1996; West, 1996), transcription termination factor Rho (Geiselmann et al., 1993), yeast PCNA and DNA polymerase III holoenzyme (Herendeen et al., 1992), and SV40 large T antigen (San Martin et al., 1997), have been shown to form hexameric rings. Six copies of pRNA form a hexameric complex. Therefore, hexamer formation is not a solitary case when fast movement of DNA or RNA is concerned. Fast movement of a protein (or protein/RNA) complex along DNA or RNA is characteristic of this group and reoccurrence of hexameric complexes within this group may give clues to their mode of action. Is it possible that hexameric complexes provide maximum capacity, interface, and stability at the same time, such that nature chooses this strategy to handle situations where rapid motion is required? It would be intriguing to find that pRNA could play a role similar to the one a protein enzyme plays.

Experimental Procedures

Synthesis of pRNA, Assay of pRNA Activity, and In Vitro Assembly of ϕ29 Virion

Methods for pRNA synthesis (Zhang et al., 1994, 1995a) and construction of circularly permuted pRNAs (Zhang et al., 1995c, 1997) have been described previously. The sequences of mutant pRNAs were confirmed by primer extension.

We have been able to assemble infectious ϕ29 virions in vitro using cloned gene products as well as synthetic pRNA and genomic DNA-gp3 (Lee and Guo, 1995). The activities of pRNAs were indicated as the ability to participate in the assembly of infectious virions in vitro, expressed as plaque-forming units per milliliter (pfu/ml), in the presence of other required components for ϕ29 assembly. The pRNA transcribed in vitro was attached to purified procapsids in the presence of Mg^{++} (Guo et al., 1991b; Chen and Guo, 1997b). Genomic DNA was subsequently packaged into the RNA-enriched procapsids with the aid of ATP and the purified DNA packaging enzyme (gp16) (Guo et al., 1986). The DNA-filled capsids were converted into infectious virions in vitro with the addition of tail protein (gp9), neck proteins (gp11) and (gp12), and morphogenic factor (gp13), which were also produced from cloned genes. Typically, 10^7–10^8 pfu/ml was obtained with wild-type pRNA, and omission of pRNA or any one of the other components resulted in no plaque formation. The synthesis of 10^8 pfu/ml of infectious virions in vitro with zero background using purified components provides a system with a sensitivity of eight orders of magnitude for assaying pRNA activity. The purification of procapsids (Guo et al., 1991a, 1991b), gp16 (Guo et al., 1986), and DNA-gp3, and the preparation of neck and tail protein extracts (Lee and Guo, 1995) have been described previously.

Stoichiometry Determination

The procedure for the determination of pRNA stoichiometry by competition inhibition of in vitro ϕ29 assembly with mutant pRNAs and for theoretical curve prediction has been described (Trottier and Guo, 1997). Briefly, ϕ29 was assembled in vitro with three pRNAs: A–b′, B–a′, and B–a′CCA. A–b′ and B–a′ were transcomplementary active pRNAs while B–a′CCA was inactive in DNA packaging due to the elimination of the essential $C_{18}C_{19}A_{20}$ bulge. As reported previously (Zhang et al., 1997), pRNA B–a′CCA would inhibit DNA packaging by competing with pRNA B–a′ for binding to procapsids while pRNA A–b′ CCA would perform likewise by competing with pRNA A–b′.

Since multiple copies of pRNA bind to each procapsid, the probability of a procapsid containing a certain number of each type of "active" and a certain number of "inactive" pRNA (for reactions containing pRNAs A–b′, B–a′, and B–a′CCA) could be calculated using the equation:

$$(p+q)^T=\binom{T}{0}p^T+\binom{T}{1}p^{T-1}q+\binom{T}{2}p^{T-2}q^2+\ \ldots\ +\binom{T}{T-1}pq^{T-1}+\binom{T}{T}q^T=\sum_{M=0}^{T}\binom{T}{M}p^{T-M}q^M$$

where p and q are the percentages of B–a′CCA and B–a′, respectively, T is 50% of the total number, Z, of pRNA per procapsid (since each procapsid is proposed to have 50% A–b′ and 50% B–a′), and M is the number of B–a′CCA bound to one procapsid. The binding of pRNA A–b′ was supposed to be equal to that of B–a′ plus B–a′CCA as its binding was unaffected by the presence of pRNA B–a′CCA. The calculated probability was extrapolated to predict the yield of pfu/ml produced in each in vitro ϕ29 assembly reaction. The yield of virions from empirical data was plotted and compared

to a series of predicted curves to find a best-fit. Predicted curves were generated by varying values for p and q. Z was presumed to be either 6 or 12.

Acknowledgments

This work was supported by grant MCB-9723923 from the National Science Foundation and grant GM48159 from the National Institutes of Health. K. G. and C. C. are recipients of the Frederick Andrews Fellowship.

Received March 20, 1998; revised May 4, 1998.

References

Bailey, S., Wichitwechkarn, J., Johnson, D., Reilly, B., Anderson, D., and Bodley, J.W. (1990). Phylogenetic analysis and secondary structure of the *Bacillus subtilis* bacteriophage RNA required for DNA packaging. J. Biol. Chem. *265*, 22365–22370.

Chen, C., and Guo, P. (1997a). Sequential action of six DNA-packing pRNAs during phage ϕ29 genomic DNA translocation. J. Virol. *71*, 3864–3871.

Chen, C., and Guo, P. (1997b). Mg^{++}-induced conformational change of packaging RNA for procapsid recognition and binding during phage ϕ29 DNA encapsidation. J. Virol. *71*, 495–500.

Davis, L.I. (1995). The nuclear pore complex. Annu. Rev. Biochem. *64*, 865–896.

Doering, C., Ermentrout, B., and Oster, G. (1995). Rotary DNA motors. Biophys. J. *69*, 2256–2267.

Dubé, P., Tavares, P., Lurz, R., and van Heel, M. (1993). The portal protein of bacteriophage SPP1: a DNA pump with 13-fold symmetry. EMBO J. *12*, 1303–1309.

Egelman, E.H. (1996). Homomorphous hexameric helicases: tales from the ring cycle. Structure *4*, 759–762.

Garver, K., and Guo, P. (1997). Boundary of pRNA functional domains and minimum pRNA sequence requirement for specific connector binding and DNA packaging of phage ϕ29. RNA *3*, 1068–1079.

Geiselmann, J., Wang, Y., Seifried, S.E., and von Hippel, P.H. (1993). A physical model for the translocation and helicase activities of *Escherichia coli* transcription termination protein Rho. Proc. Natl. Acad. Sci. USA *90*, 7754–7758.

Grimes, S., and Anderson, D. (1990). RNA dependence of the bacteriophage ϕ29 DNA packaging ATPase. J. Mol. Biol. *215*, 559–566.

Guo, P., Grimes, S., and Anderson, D. (1986). A defined system for in vitro packaging of DNA-gp3 of the *Bacillus subtilis* bacteriophage ϕ29. Proc. Natl. Acad. Sci. USA *83*, 3505–3509.

Guo, P., Bailey, S., Bodley, J.W., and Anderson, D. (1987a). Characterization of the small RNA of the bacteriophage ϕ29 DNA packaging machine. Nucleic Acids Res. *15*, 7081–7090.

Guo, P., Erickson, S., and Anderson, D. (1987b). A small viral RNA is required for in vitro packaging of bacteriophage ϕ29 DNA. Science *236*, 690–694.

Guo, P., Peterson, C., and Anderson, D. (1987c). Prohead and DNA-gp3-dependent ATPase activity of the DNA packaging protein gp16 of bacteriophage ϕ29. J. Mol. Biol. *197*, 229–236.

Guo, P., Erickson, S., Xu, W., Olson, N., Baker, T.S., and Anderson, D. (1991a). Regulation of the phage ϕ29 prohead shape and size by the portal vertex. Virology *183*, 366–373.

Guo, P., Rajogopal, B., Anderson, D., Erickson, S., and Lee, C. (1991b). sRNA of bacteriophage ϕ29 of *B.subtilis* mediates DNA packaging of ϕ29 proheads assembled in *E. coli*. Virology *185*, 395–400.

Guo, P., and Trottier, M. (1994). Biological and biochemical properties of the small viral RNA essential for the packaging of the double-stranded DNA of phage ϕ29. Semin. Virol. *5*, 27–37.

Hendrix, R.W. (1978). Symmetry mismatch and DNA packaging in large bacteriophages. Proc. Natl. Acad. Sci. USA *75*, 4779–4783.

Herendeen, D.R., Kassavetis, G.A., and Geiduschek, E.P. (1992). A transcriptional enhancer whose function imposes a requirement that proteins track along DNA. Science *256*, 1298–1303.

Ibanez, C., Garcia, J.A., Carrascosa, J.L., and Salas, M. (1984). Overproduction and purification of the connector protein of *Bacillus subtilis* phage ϕ29. Nucleic Acids Res. *12*, 2351–2365.

Jimenez, J., Santisteban, A., Carazo, J.M., and Carrascosa, J.L. (1986). Computer graphic display method for visualizing three-dimensional biological structures. Science *232*, 1113–1115.

Krug, R.M. (1993). The regulation of export of mRNA from nucleus to cytoplasm. Curr. Opin. Cell Biol. *5*, 944–949.

Lee, C.S., and Guo, P. (1995). *In vitro* assembly of infectious virions of ds-DNA phage ϕ29 from cloned gene products and synthetic nucleic acids. J. Virol. *69*, 5018–5023.

Michaud, G., Zachary, A., Rao, B., and Black, L. (1989). Membrane-associated assembly of a phage T4 DNA entrance vertex structure studied with expression vectors. J. Mol. Biol. *209*, 667–681.

Pfeifer, K., Weiler, B.E., Ugarkovic, D., Bachmann, M., Schroder, H.C., and Muller, W.E. (1991). Evidence for a direct interaction of Rev protein with nuclear envelope mRNA-translocation system. Eur. J. Biochem. *199*, 53–64.

Reid, R.J.D., Bodley, J.W., and Anderson, D. (1994a). Characterization of the prohead-pRNA interaction of bacteriophage ϕ29. J. Biol. Chem. *269*, 5157–5162.

Reid, R.J.D., Zhang, F., Benson, S., and Anderson, D. (1994b). Probing the structure of bacteriophage ϕ29 prohead RNA with specific mutations. J. Biol. Chem. *269*, 18656–18661.

Rishovd, S., Marvik, O.J., Jacobson, E., and Lindqvist, B.H. (1994). Bacteriophage P2 and P4 morphogenesis: identification and characterization of the portal protein. Virology *200*, 744–751.

San Martin, M.C., Gruss, C., and Carazo, J.M. (1997). Six molecules of SV40 large T antigen assemble in a propeller-shaped particle around a channel. J. Mol. Biol. *268*, 15–20.

Trottier, M., Zhang, C.L., and Guo, P. (1996). Complete inhibition of virion assembly *in vivo* with mutant pRNA essential for phage ϕ29 DNA packaging. J. Virol. *70*, 55–61.

Trottier, M., and Guo, P. (1997). Approaches to determine stoichiometry of viral assembly components. J. Virol. *71*, 487–494.

Tsuprun, V., Anderson, D., and Egelman, E.H. (1994). The Bacteriophage ϕ29 head-tail connector shows 13-fold symmetry in both hexagonally packed arrays and as single particles. Biophys. J. *66*, 2139–2150.

Turnquist, S., Simon, M., Egelman, E., and Anderson, D. (1992). Supercoiled DNA wraps around the bacteriophage ϕ29 head-tail connector. Proc. Natl. Acad. Sci. USA *89*, 10479–10483.

West, S.C. (1996). DNA helicases: new breeds of translocating motors and molecular pumps. Cell *86*, 177–180.

Wichitwechkarn, J., Bailey, S., Bodley, J.W., and Anderson, D. (1989). Prohead RNA of bacteriophage ϕ29: size, stoichiometry and biological activity. Nucleic Acids Res. *17*, 3459–3468.

Zhang, C.L., Lee, C., and Guo, P. (1994). The proximate 5′ and 3′ ends of the 120-base viral RNA (pRNA) are crucial for the packaging of bacteriophage ϕ29 DNA. Virology *201*, 77–85.

Zhang, C.L., Garver, K., and Guo, P. (1995a). Inhibition of phage ϕ29 assembly by antisense oligonucleotides targeting viral pRNA essential for DNA packaging. Virology *211*, 568–576.

Zhang, C.L., Tellinghuisen, T., and Guo, P. (1995b). Confirmation of the helical struture of the 5′/3′ termini of the essential DNA packaging pRNA of phage ϕ29. RNA *1*, 1041–1050.

Zhang, C.L., Trottier, M., and Guo, P.X. (1995c). Circularly permuted viral pRNA active and specific in the packaging of bacteriophage ϕ29 DNA. Virology *207*, 442–451.

Zhang, C.L., Tellinghuisen, T., and Guo, P. (1997). Use of circular permutation to assess six bulges and four loops of DNA-packaging pRNA of bacteriophage ϕ29. RNA *3*, 315–322.